Available online at www.sciencedirect.com

ScienceDirect

Procedia Environmental Sciences 4 (2011) 228–238

Procedia Environmental Sciences

Urban Environmental Pollution 2010

Study of mist-cooling for semi-enclosed spaces in Osaka, Japan

Craig Farnham[a]*, Masaki Nakao[a], Masatoshi Nishioka[a], Minako Nabeshima[a], Takeo Mizuno[b]

[a]*Osaka City University, Graduate School of Engineering, 3-3-138 Sugimoto, Osaka 558-8585, Japan*
[b]*H. Ikeuchi & Co, Ltd.,1-15-15Awaza Chuo-ku, Osaka 550-0011, Japan*

Received date September 30, 2010; revised date January 30, 2011; accepted date January 30, 2011

Abstract

Evaporative mist cooling systems are increasingly used in Japan to cool urban spaces as a counter to the urban heat island problem. Japan has a humid climate, which reduces evaporation. The balance between cooling and undesirable wetting requires careful control and placement of misting nozzles. Spraying from varying heights in an atrium showed that a single spray nozzle with Sauter mean droplet diameter of 41 microns can provide cooling of 0.7K without wetting. Cooling effects of mists with larger droplet diameters that cause slight wetting cannot be accurately measured due to the wet bulb effect on the sensors. Simulations suggest actual air temperatures are higher than wet sensor readings. Calculations of effective temperature ET* show that increases in humidity do not overcome the increase in thermal comfort due to the temperature reductions from fine mist.

Keywords: mist, evaporative cooling, heat island, spray nozzle, urban spaces

1. Introduction

Overhead hydraulic misting nozzles, producing droplets with average diameter of below 100 microns, are increasingly being used in Japan to cool urban spaces. The evaporation rates and cooling effects in a large atrium were measured for 3 nozzles at 2 operating pressures yielding flow rates ranging from 38 to 660 ml/min and Sauter mean diameters of 41 – 79 microns. Single nozzles were pointed downward, perpendicular to the floor at heights ranging from 6 – 25 m. Evaporation rates were measured by capturing the unevaporated portion of spray reaching waterproof vinyl tarps placed on the floor and weighing it. The purpose was to find the height at which these nozzles could provide cooling without wetting the floor in the still air of the atrium. For the cases of minimal and zero wetting, trials were run again and the cooling effect was measured with a grid of thermocouples.

Hydraulic nozzles, driven by high-pressure water pumps, were chosen as they are more energy-efficient than pneumatic nozzles driven by compressed air. The pump used in this paper can supply 250 L/h of water at 5.5 MPa while drawing up to 750W of electricity. The cooling potential of an evaporative system driven by this pump, given the latent heat of evaporation of water as 2450 kJ/kg at 30ºC, is 170 kW.

* Corresponding author. Tel.: +81-06-6605-2993; fax: +81-06-6605-2993.
E-mail address: craig.farnham@gmail.com.

1878-0296 © 2011 Published by Elsevier Open access under CC BY-NC-ND license.
doi:10.1016/j.proenv.2011.03.027

1.1. Evaporative Mist Cooling Background

Evaporative spray cooling systems have been used successfully in arid climates such as Spain by Alvarez et al. [1] and in cooling towers in Israel with coarse sprays by Pearlmutter et al. [2] with temperature reductions of as much as 15K. Japan's humid climate causes lower evaporation rates than in such arid climates, making the use of such coarse sprays impractical. In urban areas, it is important that spray cooling systems do not cause wetting of the people and surfaces beneath. Use of fine mists sprayed from overhead nozzles to cool outdoor pedestrian spaces at the Aichi Expo 2005 by Yamada et al. [3] yielded cooling of 2-3K. Uchiyama et al. [4] conducted surveys of people experiencing an overhead fine mist spray cooling system at a rail platform which showed that 77% of people claimed increased thermal comfort even with a measured cooling effect of only 1-2K on a 34ºC day, but 53% felt slight (38%) or significant (15%) wetting. Pooling of water on surfaces below is not desired as it can be seen as a safety hazard. Alvarez et al. see pooling as both a waste of water, and reducing the cooling effect of the mist as humidity is increased by evaporation from pooled water which may not yield as much cooling. The balance between optimizing cooling and minimizing wetting of people and surfaces under the nozzles is a key concern.

1.2. Climate and Infrastructure of Osaka

Osaka, Japan has a humid subtropical climate according to the Koppen climate classification in the recent map by Peel et al. [5] In an average of the past 5 years (2005-2009) shown in Figure 1 at left, the average daily high temperature peaks at 33.6°C in August, while relative humidity averages from 60-70%. Over the past century, average daily temperatures and average daily high temperatures have risen about 2°C, while average relative humidity has fallen from 75% to around 65% as shown in Figure 1 at right, according to data from the Japan Meteorological Agency [6]. Osaka is also particularly noted in Japan for the phenomenon named *nettaiya* (Lit. "tropical nights") in which the nightly low temperature does not drop below 25C. This is one form of the urban heat island effect, which has steadily grown stronger with the annual number of *nettaiya* in Osaka surpassing 40 nights each year since the year 2000 where it had averaged around 10 nights per year in the 1930s according to data from the Japan Meteorological Agency.

Mist cooling for the human environment requires a clean water supply. Osaka's water supply is chlorinated to 5mg/L in the mains, and tap water is maintained at a level of 1mg/L as per Osaka City Water Bureau regulations [7]. According to [8] this level is sufficient to kill *legionella* bacteria within 40 minutes at 21°C, and faster at higher temperatures.

Osaka is located on the Pacific coast and is found on the Kinki Plain, with several rivers running into Osaka Bay and the nearby Lake Biwa providing fresh water. Covered urban shopping arcades are common throughout the city, many over 1 kilometer in length. These semi-enclosed spaces could be well-suited for mist cooling systems, as they are fairly sheltered from scattering winds, while openings to outside air at intersections and alleyways should prevent humid air from accumulating and degrading performance.

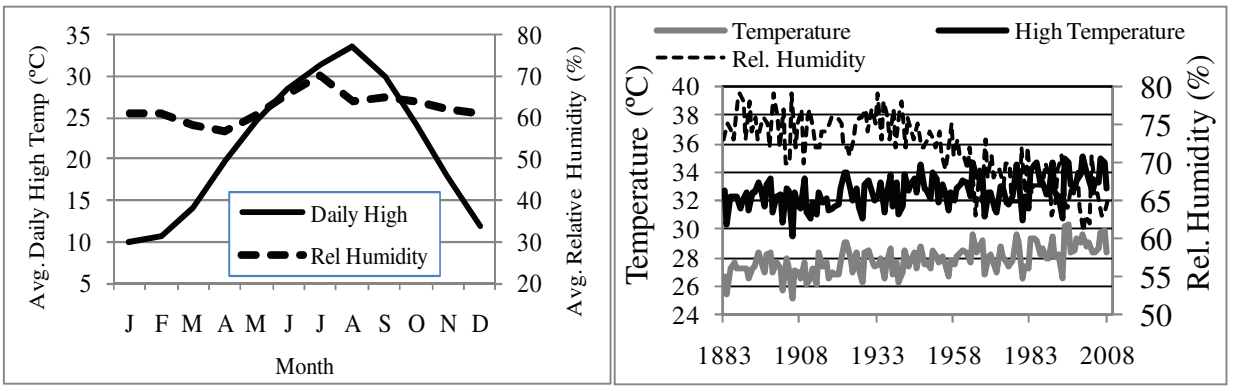

Figure 1 Osaka climate data. 5-year monthly average from 2005-2009 (Left). Annual averages for August (Right).

2. Procedure

Three models of hydraulic nozzle were evaluated at 2 operating pressures. In each trial, a single nozzle was connected to a high-pressure water pump, supplying water at 0.7MPa or 5.5MPa. Nozzle droplet size distributions were measured with a PDPA (Phased-Doppler Particle Analyzer). PDPA diameter distribution measurements were taken along the centerline of the spray, 50cm below the nozzle, with the nozzle oriented straight down. Diameter distribution data were processed to yield the Sauter Mean Diameter (SMD) as shown in Table 1. Nozzle flow rates were measured by placing a beaker over the nozzle for 120 seconds and measuring the weight of accumulated water.

Table 1 Nozzle spray properties

Nozzle	Pressure (MPa)	Flow rate (L/hr)	SMD (μm)
A	0.7	3.0	58
B	0.7	7.4	65
C	0.7	15.1	79
A	5.5	10.9	41
B	5.5	19.5	45
C	5.5	40.0	55

The evaporation rate of the mist as a whole was measured. In all trials, a single nozzle was suspended above the chamber floor pointing down at differing heights, *z*. A small bucket was suspended just under the nozzle and the pump turned on. After the pump reached the spraying pressure of 0.7 or 5.5 MPa, a timer was started and the bucket removed. Mist sprayed downward and evaporated as it descended to the floor. The unevaporated potion of the mist was captured on a waterproof vinyl tarp which had been weighed while dry. After the set time (5 minutes, regularly changed to 10 minutes to confirm time dependency was minimal) the bucket was repositioned under the nozzle to block the mist. The pump was then turned off. Pressure remaining in the piping to the nozzle causes continued and coarsening spraying for a few seconds. This was blocked by the bucket. The tarp was then folded from the outside inward within 30 seconds of the end of the misting period to minimize secondary evaporation off the tarp, placed in a large bucket and weighed. The procedure is illustrated in Figure 2 (Left).

Environmental conditions were measured with electronic temperature/humidity loggers housed in ventilated weather shelters placed 3m distant from the centerline of the mist spray cone at 1m, 13m and 25m height. A fourth sensor with no weather shelter was placed 20 cm horizontally from the nozzle. The loggers are rated as accurate to +/- 0.5ºC for temperatures from 0ºC to 50ºC and +/- 5%RH for relative humidity from 10% to 95%. Loggers recorded temperature and relative humidity every 10 seconds. Environmental conditions were taken as the average of the 4 loggers at the moment the misting pump was switched on for each trial.

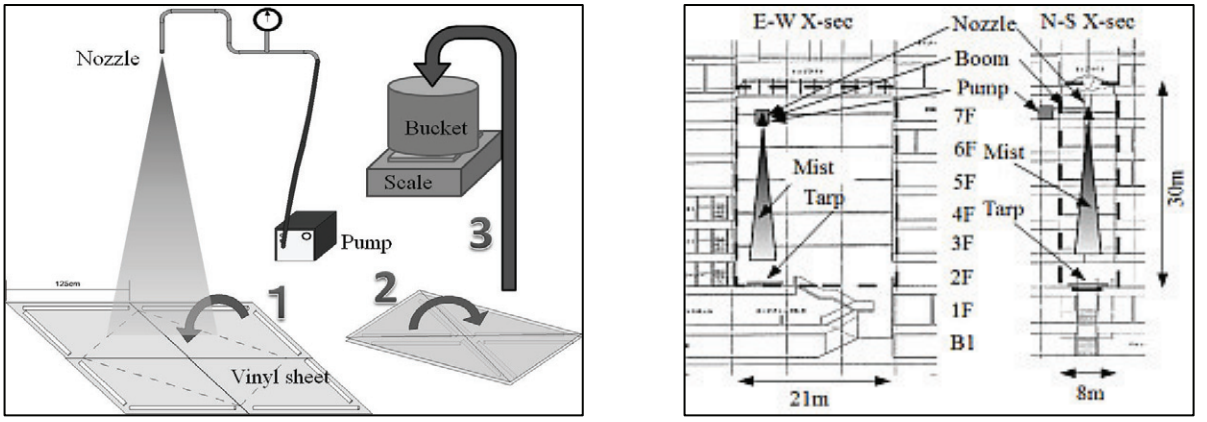

Figure 2 Procedure for measurement of evaporation rate (Left). Atrium cross-sections and equipment (Right)

Directly measuring the cooling effect inside a mist spray is difficult. Preliminary experiments had the same result, each sensor slowly became wet and tended to reach the wet bulb temperature over 1 – 10 minutes. For cases in which the mist nearly or completely evaporated before reaching the floor, it was expected the sensors would not become wet. The experiments were repeated at the same conditions on the same night. A 2m X 2m frame forming a 2-dimensional grid of 16 T-type thermocouples in a 4X4 pattern spaced at intervals of 50cm was suspended 1m above the floor centered below the nozzle for horizontal temperature distributions, or propped up perpendicularly in contact with the floor for vertical temperature distributions. The thermocouples were connected to a digital data logger which recorded temperatures every second. The digital temperature/humidity logger sensor was placed at the edge of the frame to more closely measure the humidity change due to the mist. The spraying procedure was repeated without the vinyl tarps, and spraying time was 6 minutes in each case.

2.1 Test Site

Trials were done in a large atrium 20m X 8m X 30m high. The atrium is partially-open at the bottom, with a large stairwell (8m X 20m) leading down through two levels (see Figure 1, Right) to the basement. These two levels are 38m X 64m X 4.5m height. The nozzle was centered over the upper landing (8m X 10m) of this stairwell. Trials in the large atrium were done overnight while the building was closed, to reduce any natural convection effects. All ventilation systems were turned off in the test areas. Most lighting was also turned off to reduce any convection effects and to aid in making visual confirmation that the mist cone did not stray outside the tarp area. When laying out tarps for the first run of each evening, one person stood at each corner of the tarp with a flashlight, while another stood at the other corner along the same edge and confirmed no mist was passing through the flashlight beam.

3. Mist Evaporation

Pruppacher and Klett [9] found that the rate of evaporation of water droplets in air in common atmospheric conditions is largely a function (Eq. 1) of the wet bulb depression, ΔT_{WB} (the difference between the dry and wet bulb temperatures) as the surface temperature of evaporating water droplets, T_w is usually within +/- 0.5K of the wet bulb temperature. In terms of droplet mass and size, the relation is:

$$\Delta T_{WB} \approx T_w - T_a = -\frac{L}{4\pi A k_a}\left(\frac{dm}{dt}\right) \tag{1}$$

where A is the droplet surface area, k_a is the thermal conductivity of air, L is the latent heat of evaporation of water, T_a is the dry bulb temperature, dm/dt is the rate of change of mass of the droplet and the other variables are as above. This individual droplet relationship was also was found to correlate empirically by the authors, Farnham et al. [10] with the net evaporation rate of mist cones as measured by the experimental technique in this paper. The wet bulb depression, ΔT_{WB} was found to be useful as a quick reference to compare the evaporation potential of different weather conditions. A greater value indicates greater potential for evaporation, while also likely indicating the maximum possible cooling effect.

3.1. Mist Simulation with Fire Dynamics Simulator

As measuring temperatures and humidity inside a mist cone are difficult, simulations were done to provide some sense of the change of temperature and humidity within the mist cone. Simulation results can also be compared to wet sensor readings.

The Fire Dynamics Simulator (FDS) is a public-domain software package first released in 2000 and under continuous development by the National Institute of Standards and Technology (NIST) of the United States [11]. FDS Version 5.5, Build 6004 with multi-thread processing for 64-bit operating systems was used here. It is bundled with a separate visualization program, Smokeview. FDS calculates over a user-defined rectilinear grid. Flow is solved numerically using a form of the Navier-Stokes equations appropriate for low-speed, thermally-driven flow. Turbulence is handled by the Smagorinsky form of Large Eddy Simulation (LES). Particles, including water droplets, are handled as Lagrangian points traveling through the Eulerian grid elements which handle air flow.

Although FDS is almost exclusively used to analyze structural fires and smoke ventilation, there are many related functions, including the ability to model water sprinklers. By setting a simulation to avoid the default spray parameters, fine mist cooling simulations can be performed. FDS has not been validated for use as a mist cooling system model. If dry sensor readings in this experiment match the simulation, but wet sensor readings are cooler than the simulation, it could mean that the simulation reflects the actual air temperature at the sensor, and the difference is due to the wet bulb effect. Further study is needed to confirm this.

3.2. Thermal Comfort

Evaporative mists can reduce air temperature, but at the cost of increasing humidity. Indices of thermal comfort account for several factors including humidity. The Effective Temperature, ET*, as defined by ASHRAE [12] in Equation 2, can quantify these effects. An ET* value at an observed temperature and relative humidity level equates to the thermal comfort experienced at a relative humidity of 50% and an operative temperature equal to the ET* value.

$$ET^* = T_o + wi_m LR\left(P_a - 0.5P_{ET^*,sat}\right) \quad (2)$$

where T_o is the operative temperature, in this case assumed to be equal to the temperature of the semi-enclosed space where the radiative temperature and air temperature are equal, w is the skin wettedness ratio, for this model a value typical at these conditions as per ASHRAE $w = 0.2$ is used, i_m is the total vapor permeability of clothing, for these calculations the value for trousers and a short sleeve shirt, 0.43 is used, LR is the Lewis ratio of 16.5 K/kPa, P_a is the vapour pressure and $P_{ET^*,sat}$ is the saturated vapour pressure at ET*. Equation 2 was solved iteratively using an approximation for saturation vapor pressure used in the HASP/ACSS/8502 air conditioning simulation software developed by JAMBEE [13] and the Newton-Raphson method . As mist cools the air and raises humidity, the initial value of ET* and the value of ET* during misting can be compared to reveal if the perceived temperature is still lower even though the humidity has increased. If we solve for a simple difference equation of ET* before and during cooling, we find the amount by which humidity would have to be increased to cancel out the perceived cooling. As long as the increase in humidity due to misting is below this limit, there should be a perception of cooling. If the increase in humidity is greater than this limit, there will likely be a perception of increased thermal discomfort. In addition, there should be further increases in perception of cooling that may be caused by fine droplets impacting and evaporating from the skin, as well as an increase in air speed over the skin due to the downdraft generated by overhead mist nozzles.

4. Results

4.1. Evaporation Rates

A total of 34 successful trials on evaporation rates were run over 5 nights. Evaporation rates and environmental conditions in the atrium are shown in Table 2. The climate control system in the atrium building, although turned off overnight, kept temperatures between 25 and 28ºC while relative humidity ranged from 44 to 69%. The wet bulb depression ranged from 4.4K to 8.2K.

Evaporation rates tend to increase with height as shown in **Errore. L'origine riferimento non è stata trovata.**. Trials of Nozzle C at 5.5MPa were stopped after the manufacturer warned the nozzle was not designed for high pressure. There were only 2 cases of complete evaporation, both using Nozzle A at 5.5MPa. One case had the nozzle at 25m height, the second at 15m height. Another trial at 15m height with Nozzle A at 0.7MPa showed an evaporation rate of 95%, but the wet bulb depression was much smaller and SMD was larger than the 100% evaporation case. Near-complete evaporation of 99% was achieved with Nozzle B in one case at 25m.

Tests of time dependency, with spray times of 5 and 10 minutes under nearly the same conditions, showed differences of under 5% evaporation rate, with the longer spraying time always showing greater evaporation rates. This may show that secondary evaporation from the vinyl tarp has a stronger influence over time than any further

increases in humidity due to longer spray times.

Table 2 Environment Conditions and Evaporation Rates

Nozzle/Pressure	Height (m)	Avg.Temp. (ºC)	Avg. Rel. Humidity %RH	ΔT_{WB} K	Spray time (min)	Flow rate (L/hr)	Evaporation %
A 0.7MPa	6.0	27.1	55	6.6	10	2.8	58
A 0.7MPa	6.0	27.0	56	6.5	10	2.8	56
A 0.7MPa	10.5	27.7	58	6.3	10	3.1	90
A 0.7MPa	15.1	28.1	59	6.1	5	3.0	95
A 5.5MPa	6.0	24.8	47	7.5	5	12.1	66
A 5.5MPa	6.0	24.7	48	7.4	5	12.1	63
A 5.5MPa	15.1	25.5	44	8.2	5	9.9	100
A 5.5MPa	24.5	26.8	68	4.5	10	10.0	100
B 0.7MPa	6.0	26.8	58	6.1	10	7.4	43
B 0.7MPa	6.0	26.8	58	6.1	10	7.4	44
B 0.7MPa	10.5	27.7	60	5.9	5	7.3	71
B 0.7MPa	10.5	27.6	61	5.7	5	7.3	69
B 0.7MPa	15.1	28.1	59	6.0	5	7.4	91
B 0.7MPa	15.1	28.0	60	5.9	10	7.4	88
B 0.7MPa	19.7	28.1	63	5.5	10	7.5	97
B 0.7MPa	24.5	27.7	62	5.7	5	7.3	99
B 5.5MPa	6.0	24.9	47	7.7	5	20.0	51
B 5.5MPa	6.0	24.8	47	7.5	5	20.0	49
B 5.5MPa	15.1	25.2	47	7.7	10	19.2	91
B 5.5MPa	15.1	24.9	49	7.3	5	19.2	87
B 5.5MPa	24.5	26.8	69	4.4	5	19.7	93
C 0.7MPa	6.0	27.0	57	6.3	10	15.2	35
C 0.7MPa	6.0	26.9	58	6.2	10	15.2	34
C 0.7MPa	10.5	27.6	59	6.0	5	15.1	60
C 0.7MPa	10.5	27.7	60	5.9	5	15.1	59
C 0.7MPa	15.1	28.1	62	5.7	5	15.1	78
C 0.7MPa	15.1	28.0	61	5.8	10	15.1	73
C 0.7MPa	19.7	28.2	63	5.5	5	15.2	85
C 0.7MPa	19.7	28.0	64	5.3	10	15.2	82
C 0.7MPa	24.5	27.7	64	5.2	5	15.1	86
C 0.7MPa	24.5	27.3	66	4.9	10	15.1	84
C 5.5MPa	6.0	24.9	47	7.7	5	39.9	37
C 5.5MPa	15.1	24.8	51	6.9	5	40.2	66
C 5.5MPa	15.1	24.9	49	7.3	10	40.2	69

4.2. Cooling Effect

After finding the complete and near-complete evaporation cases, 4 trials were completed with the thermocouple grid to measure the cooling effect. One trial with the thermocouple grid suspended horizontally and one trial with the grid positioned vertically was done for both Nozzle A and Nozzle B at 25m height. Spraying was done for 6 minutes in each case. The average and maximum temperature drops for the 5 minutes span from 1 minute after the start of spraying until the end of spraying are shown in Table 3and Table 4. Temperature and humidity changes over time are shown in Figure 3 and Figure 4.

Temperature drops for Nozzle A were slight, averaging 0.7K during the horizontal trial and 0.5K in the vertical trial. On close visual inspection the thermocouples did not have water droplets on them. There was no significant difference between average temperature drops at different heights in the vertical distribution from 0.25m to 1.75m. This may show that there is no significant temperature gradient in the cooling effect as experienced by humans from this nozzle.

Temperature drops for Nozzle B were higher at 1.8K for the horizontal case, and 2.1K for the vertical case. Droplet formation was apparent on all thermocouples in both cases. The larger temperature drops are a result of the wet bulb effect. There was a temperature gradient in the vertical case, with the uppermost thermocouples showing the greatest drop in temperature, perhaps due to greater wetting. This may also have been influenced by the frame holding the thermocouples, which is made of 2.5cm diameter aluminum tubing, which also collected water droplets..

Table 3 Average and maximum reductions in temperature at each thermocouple for Nozzle A

Nozzle A Horizontal

		x – position (m)				
		0	0.5	1.0	1.5	Avg.
y = 0	Avg	0.6	0.4	0.5	0.7	0.5
	Max	0.9	0.8	0.7	0.9	
y = 0.5	Avg.	0.6	0.4	0.6	0.8	0.6
	Max	1.0	0.7	0.9	1.0	
y = 1	Avg.	0.5	0.6	0.3	0.4	0.4
	Max	0.7	0.9	0.7	0.6	
y = 1.5	Avg.	0.5	0.5	0.3	0.4	0.4
	Max	0.7	0.9	0.6	0.7	
		Grid Average				0.7

Nozzle A Vertical

		x – position (m)				
		0	0.5	1.0	1.5	Avg.
z = 1.75	Avg.	0.7	0.7	0.7	0.7	0.7
	Max.	0.9	0.8	0.8	0.9	
z = 1.25	Avg.	0.0	0.8	0.7	0.6	0.5
	Max.	0.8	0.9	0.9	0.8	
z = 0.75	Avg.	0.7	0.8	0.8	0.7	0.7
	Max.	0.8	1.0	1.0	0.9	
z = 0.25	Avg.	0.6	0.8	0.7	0.7	0.7
	Max.	0.8	1.0	0.9	0.9	
		Grid Average				0.5

Table 4 Average and maximum reductions in temperature at each thermocouple for Nozzle B

Nozzle B Horizontal

		x – position (m)				
		0	0.5	1.0	1.5	Avg.
y = 0	Avg	1.2	1.4	1.5	1.5	1.4
	Max	1.5	1.8	2.3	2.0	
y = 0.5	Avg.	1.7	1.7	2.0	1.7	1.8
	Max	2.4	2.2	2.7	2.2	
y = 1	Avg.	1.9	2.3	2.5	2.3	2.2
	Max	2.8	3.0	3.1	3.1	
y = 1.5	Avg.	1.5	2.0	2.2	1.9	1.9
	Max	2.2	3.0	2.7	2.6	
		Grid Average				1.8

Nozzle B Vertical

		x – position (m)				
		0	0.5	1.0	1.5	Avg.
z = 1.75	Avg.	2.2	2.2	2.3	2.1	2.2
	Max.	2.7	3.0	3.0	2.6	
z = 1.25	Avg.	2.6	1.9	2.6	2.6	2.4
	Max.	3.2	2.6	3.2	3.1	
z = 0.75	Avg.	1.9	2.3	1.8	1.7	1.9
	Max.	2.4	3.3	2.9	2.3	
z = 0.25	Avg.	1.5	1.6	1.5	1.9	1.6
	Max.	2.5	2.7	2.7	3.1	
		Grid Average				2.1

4.3. Comparison of measured cooling with FDS simulation

Due to the wetting of the thermocouples for the Nozzle B trials, the measured temperatures are likely at a point between the air temperature and the wet bulb temperature. Results from an FDS simulation run at the same conditions as the horizontal Nozzle A trial showing temperature and relative humidity cross-sections at the nozzle centerline and at 1m height at 300 seconds after mist activation are shown in Figure 5. Dark gray highlighting is added at 25.9ºC and 73.5% relative humidity to aid visualization. The simulation results have the cooling effect at 1m height as 0.7 +/- 0.2K over the area where the thermocouples were located, with humidity increasing by 3% or less. This matches the experimental measurements.

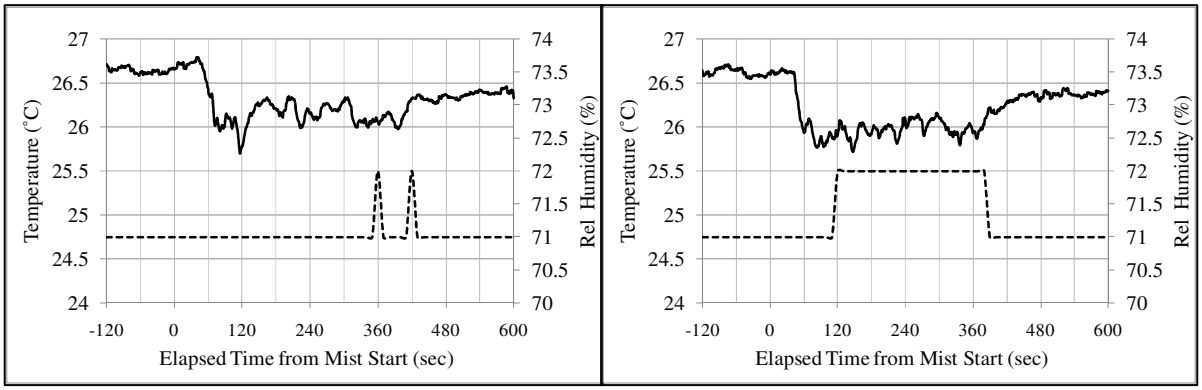

Figure 3 Measured cooling (solid line) and humidity increase (dotted line) for Nozzle A horizontal trial (left) and vertical trial (right)

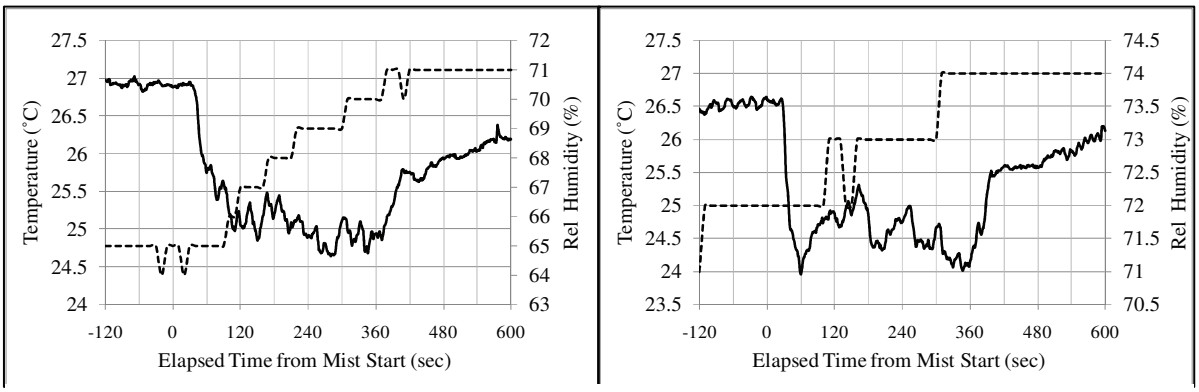

Figure 4 Measured cooling (solid line) and humidity increase (dotted line) for Nozzle B horizontal trial (left) and vertical trial (right)

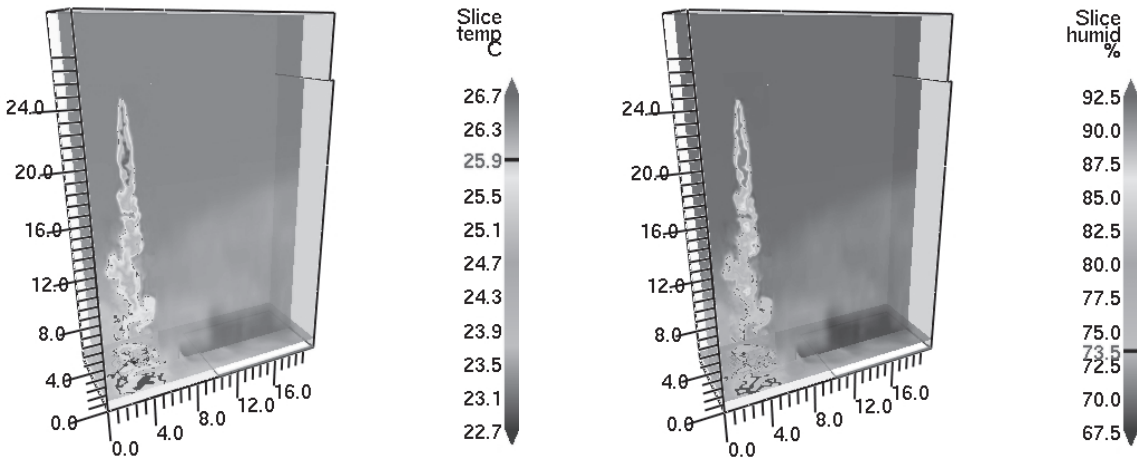

Figure 5 FDS simulation result for Nozzle A at same conditions as experimental trial. Cross sections of temperature (left) and rel. humidity (right). Note dark gray highlighting on plots and scale bars to indicate mean values at z=1 cross-section.

A simulation of conditions for the Nozzle B trials showed that the cooling effect was a drop of 1.1 +/- 0.2K at the thermocouple location, while the measured temperature drop was 1.8 +/- 0.8K. It is possible that the air temperature matches the simulation, while the measured temperature is lower due to the wet bulb effect.

4.4. Thermal Comfort

Although humidity increases slightly for Nozzle A, and more for Nozzle B, the cooling of the air outweighs the decrease in thermal comfort due to the rise in humidity. The initial temperature and relative humidity are taken as the averages of the values in the 2 minutes before spraying. The temperature drop is the average drop shown in Table 3 and Table 4. The initial value of ET* is compared to the misting value of ET*, using the maximum humidity from each trial in Table 5. In most cases, the effect of the slight increase in humidity is so small that the change in ET* is the same as the temperature drop. In the case of the largest humidity increase of 6% with Nozzle B, the drop in ET* is only slightly less (1.6K) than the air temperature drop (1.8K).

Figure 6 shows the amount by which humidity must rise to negate cooling effects of 0.5ºC, 1ºC, and 2ºC over temperatures ranging from 26ºC to 40ºC for low humidity (30%) and high humidity (60%) starting conditions. A cooling of only 0.5ºC at a low initial humidity of 30% only allows for an increase of 6-12% relative humidity, or 2.4 -2.7 g/kgDA absolute humidity before perceived cooling is lost. Further increases in humidity would yield a perceived increase in ET* and net reduction of thermal comfort. At the higher initial humidity of 60%, the limit is slightly higher. With greater levels of cooling, such as the case of 2.0ºC at 60% humidity, an increase of 40% relative humidity from 32 ºC, yielding a saturated state of 100% relative humidity, indicates that even misting in great enough amounts to raise humidity to saturation would still yield a reduction in ET* as long as the change in air temperature is 2.0ºC or greater. Simulation results tend to show that regions of such high humidity also tend to be in regions close to the nozzle where the mist cone has not fully evaporated, thus exposed skin would become wet, complicating the evaluation of thermal comfort. These areas should also tend to have air temperatures near the wet bulb temperature. Experimental confirmation is a problem, as attempts at measurements of air temperature and humidity inside the incompletely unevaporated mist cone tend to yield readings of the wet bulb temperature and 100% humidity.

Table 5 Measured cooling effect and change in thermal comfort for Nozzle A and B at 25m.

	Nozzle A		Nozzle B	
	Horizontal	Vertical	Horizontal	Vertical
Initial Avg Temp	26.3	26.6	26.9	26.5
Initial Avg Humidity	71	71	65	72
Avg temp drop	0.7	0.5	1.8	2.1
Max humidity rise	1%	1%	6%	2%
Initial ET*	27.2	27.5	27.6	27.4
Misting ET*	26.5	27.0	25.9	25.3
Reduction in ET*	0.7	0.5	1.6	2.1

5. Discussion

Single nozzles spraying mists with SMD of 41 – 45 microns can provide non-wetting or nearly non-wetting cooling in still air in a semi-enclosed space. Resultant increases in humidity have little or no effect on the thermal comfort as calculated by effective temperature, ET* as defined by ASHRAE. Mists of greater SMD will cause wetting even from heights of 25m and may not be useful for cooling urban pedestrian spaces. However, when considering application of mists in urban shopping arcades, the still air case evaluated here presents a worst-case scenario. Shopping arcades have air currents to promote evaporation of water droplets.

Calculations showing the break-even point between temperature drops and the humidity increase necessary to cancel out the drop in before-after misting ET* calculations suggest that fine cooling mists will always increase

thermal comfort in warm humid conditions even when the cooling effect is slight. However, this does not account for physical discomfort due to wetting, nor long-term humidity rises in spaces without ventilation.

Simulation indicates that wet sensors may not be yielding the accurate temperature of the cooled air, but a lower value due to the wet bulb effect. Using these readings may lead to incorrect evaluations of thermal comfort. However, many factors in mist cooling thermal comfort need investigation: including the effect of mist contact on human skin and clothing, changes in skin wettedness and the makeup of the moisture on skin changing from sweat to pure water effecting the calculation of ET*, changes in air velocity over skin due to the downdraft induced by overhead misting, and possible reductions in radiative temperature due to the mist cloud.

Experiments are currently underway to measure the evaporation rates and cooling effects of multiple nozzle arrays in semi-enclosed and outdoor environments near buildings. A validation study of FDS for mist cooling is also underway.

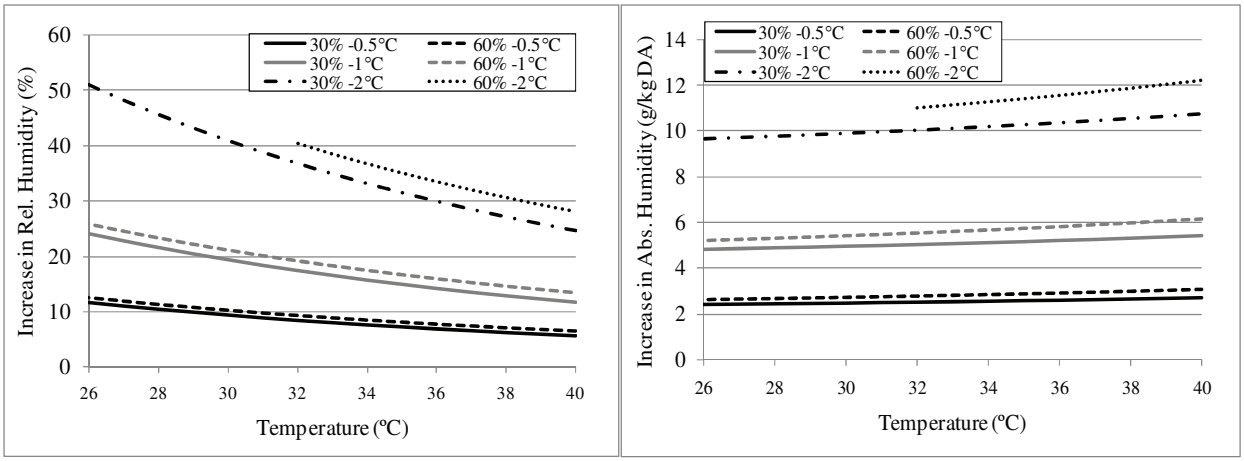

Figure 6 Break-even rise in humidity which negates perceived cooling from indicated initial conditions. Relative humidity rise (left) and absolute humidity/mixing ratio (right).

References

1. Alvarez, S., Rodriguez E.A., & Martin R. 1991. Direct air cooling from water drop evaporation. *Architecture and Urban Space*: 619-624.
2. Pearlmutter, D., Erell E., Etzion Y., Meir I.A., & Di H. 1996. Refining the use of evaporation in an experimental down-draft cool tower. *Energy and Buildings 23*: 191-197.
3. Yamada H, Okumiya M, Tsujimoto M, Harada M. (2006). Study on Cooling Effect with Water Mist Sprayer: Measurement on Global Loop at the 2005 World Exposition. *Architectural Inst. of Japan Congress*. Kanto. p. 677 [in Japanese]
4 Uchiyama S, Suzuki K, Tsujimoto S, Koizumi H. (2008). An Experiment in Reducing Temperatures at a Rail Platform. *Japan Society of Plumbing Engineers*, 25(2),2. [in Japanese]
5. Peel M, Finlayson B, McMahon T. (2007). Updated world map of the Köppen-Geiger climate classification. *Hydrol. Earth Syst. Sci.* 11: pp. 1633-1644.
6. Japan Meteorological Agency (retrieved 2010) http://www.jma.go.jp/jma/indexe.html
7. Osaka City Waterworks Bureau 2008. *Water Quality Management.* www.city.osaka.jp/suido/english/quality/ check/qa. html.
8. Kuchta, J, States S. McNamara A, Wadowsky R., Yee R. (1983). Susceptibility of *legionella pneumophilia* to chlorine in tap water. *Applied and Environmental Microbiology Vol. 46, No. 5:* pp. 1134-1139.
9 . Pruppacher H, Klett J. (1997). *Microphysics of clouds and precipitation*. Dordrecht: Kluwer Academic Publishers.

10. Farnham C, Nakao M, Nishioka M, Nabeshima M, Mizuno T. (2009) A Proposal for Mist Cooling Control and Measurement Methods. *Trans. Of the JSRAE*. Vol. 26, No. 1. Pp. 105-112. [in Japanese]
11. United States. NIST. (2007) *Special Publication 1018-5 : Fire Dynamics Simulator User Guide and Technical Reference Guide*. Washington: US Government Printing Office.
12. ASHRAE (2005). *ASHRAE Handbook – Fundamentals*. *Ch. 8 Thermal Comfort.* Atlanta.
13. Japan Building Mechanical and Electrical Engineers Assoc. (1992). *HASP/ACSS/8502 Program Manual*. Tokyo. (in Japanese).